Models of Extended Gravitational Lenses

Christopher S. Kochanek

Harvard-Smithsonian Center for Astrophysics, Cambridge, MA 02138, USA

FERMILAB
NOV 22 1993
LIBRARY

Fermilab Library
0 1160 0035056 5

CFA-3 7178

Abstract: There are three methods for accurately inverting extended gravitational lenses: the Ring Cycle algorithm, LensClean, and MEM for lenses. I outline the issues in inverting extended lenses and show an application to the radio ring MG1654+134. Isothermal models adequately fit the X band map of MG1654+134, while more centrally concentrated models, such as the Plummer model, cannot. The upper limit on the core radius of the isothermal model is $s \lesssim 0\farcs15$, or $370h^{-1}$ pc in an Einstein-DeSitter cosmology.

1 Introduction

There are three objectives in modeling gravitational lenses. The first is to produce a model for the mass distribution of the lens, the second is to produce a model of the intrinsic source structure, and the third is to do the modeling with a procedure that provides an objective estimate for how well the model fits the data and allows estimates of errors in the model. A model without objective measures of how well it fits the data leaves no means for outsiders to judge the quality of the inversion and makes it difficult to compare different inversions. In the absence of error bars, there is no way to estimate the significance of the estimated parameters or the uniqueness of the model.

The inversions of multiply imaged quasars are greatly simplified by the simple structure of the source and the small number of constraints that must be satisfied. However, most of the observed lens systems are formed by multiply imaging either extended radio sources (discussed by Patnaik) or distant galaxies (discussed by Hammer and Soucail). Unlike the point image systems formed by multiply imaging quasars, it is sometimes difficult to recognize the parts of the image that originate from the same source point. Yet most of the constraints on the lens model in these systems come from the extended structure rather than the compact emission. Inverting these systems requires methods that correctly weight the importance of the various parts of the image. There are three systematic approaches to inverting these systems: the Ring Cycle algorithm (Kochanek *et al* 1987), LensClean (Kochanek & Narayan 1992), and MEM for lenses (discussed by Wallington).

In the extended lenses, the only objective measure of whether a model is consistent with the lens data is the degree to which the model is consistent with the observed image. All three methods work on the same principle. For any lens model, there is a well defined best fit source structure defined by back-projecting the observed image through the existing model. The error in the model is the difference between the observed image and the model image of the best fit

source. This defines a χ^2 measure for the goodness of fit as the mean square difference between the observed image and the model image of the best fit source normalized by the estimated noise level in the data. A good fit is found when the differences between the observed image and the model image are compatible with the noise.

2 LensClean

LensClean (Kochanek & Narayan 1992) builds on the Clean algorithm of radio astronomy (Högbom 1974, Clark 1980) by using the *ansatz* that all radio sources can be minimally decomposed into a pattern of point sources. Clean is an iterative process in which you find the peak of the image (the "dirty" map), subtract an image of the telescope point spread function (the "dirty" beam) with a fraction γ (the "gain") of the flux at that point, and add a point component with the same flux to a new "clean" map. The procedure is repeated until the dirty map is reduced to the noise level of the observation. The clean map is then convolved with a clean beam that has the same resolution as the observation but lacks the complicated sidelobe pattern of the dirty beam and the residuals are added to produce the final map.

Where Clean places the point components in the image plane of the lens, LensClean places them in the source plane of the lens. Thus, in regions that are singly imaged, the two methods are identical, but in multiply imaged regions, LensClean can subtract all the flux from the dirty map only if it has the correct lens model. This defines the error measure in LensClean to be the residuals in the dirty map compared to the residuals from a normal Clean. Once we can estimate the error for any given lens model, we then adjust the parameters of the model to minimize the error. A model is compatible with the data when the χ^2 residual is compatible with the number of degrees of freedom in the map. The variations in the χ^2 for small changes in the parameters allow us to estimate errors on the parameters near the best fit model.

3 An Example: MG1654+134

The radio ring MG1654+134 was the second ring discovered (Langston *et al* 1989). We discuss an inversion of MG1654+134 using an elliptical singular isothermal sphere truncated at quadrupole order,

$$\phi = br + \epsilon br \cos 2(\theta - \theta_\epsilon),$$

corresponding to surface density

$$\Sigma \propto \frac{b}{r}\left(1 - 3\epsilon \cos 2(\theta - \theta_\epsilon)\right),$$

where b is the unperturbed critical radius, 3ϵ is the ellipticity of the surface density, and θ_ϵ is the orientation angle of the minor axis of the surface density measured West to North. The peak and rms noise levels in the original map are 130μJy and $\sigma_0 = 30\mu$Jy respectively compared to the peak of the map of 4700μJy. We estimate that the number of degrees of freedom in the inversion is $\nu \simeq 400$. If the LensClean inversion has rms residuals σ the estimated $\chi^2 = \nu(\sigma/\sigma_0)^2$. The best fit model has rms residuals of 24μJy and peak residuals of 190μJy, slightly better and worse respectively than the noise levels. The X band image, the LensClean reconstruction, the inferred source, and the residuals are shown in figure 1.

The model has five parameters $p_i = \{b, x_l, y_l, \epsilon\cos 2\theta_\epsilon, \epsilon \sin 2\theta_\epsilon\}$ when we include the lens position (x_l, y_l). The values at the minimum of the χ^2 are $b = 1\farcs000$, $\epsilon\cos 2\theta_\epsilon = -0.058$, and $\epsilon \sin 2\theta_\epsilon = -0.027$, and the lens position is marked in the figure. If we fit the error surface near

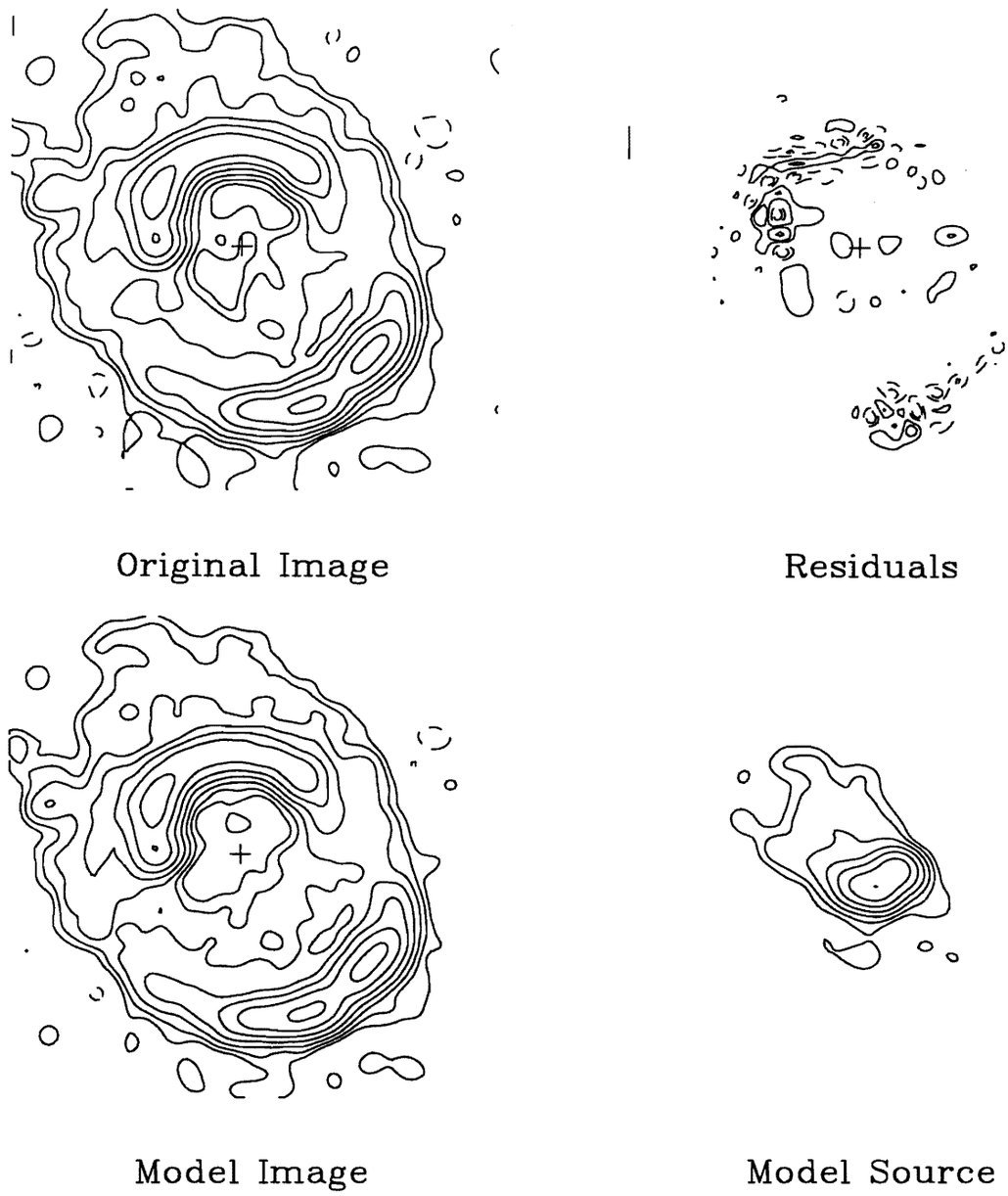

Figure 1: Original X band map, reconstructed map, reconstructed source, and residuals for the radio ring MG1654+134. In a perfect reconstruction the original and reconstructed maps would be identical up to a residual pattern at the level of the noise in the observations. The + marks the position of the lens. The contours are logarithmically spaced at -100 and -50 μJy (dashed lines) and 50, 100, 200, 400, 800, 1600, and 3200 μJy (solid lines). The quasar producing the jets that power the lensed lobe lies to the North-East. Only the 50 and 100 μJy contours appear in the residuals map.

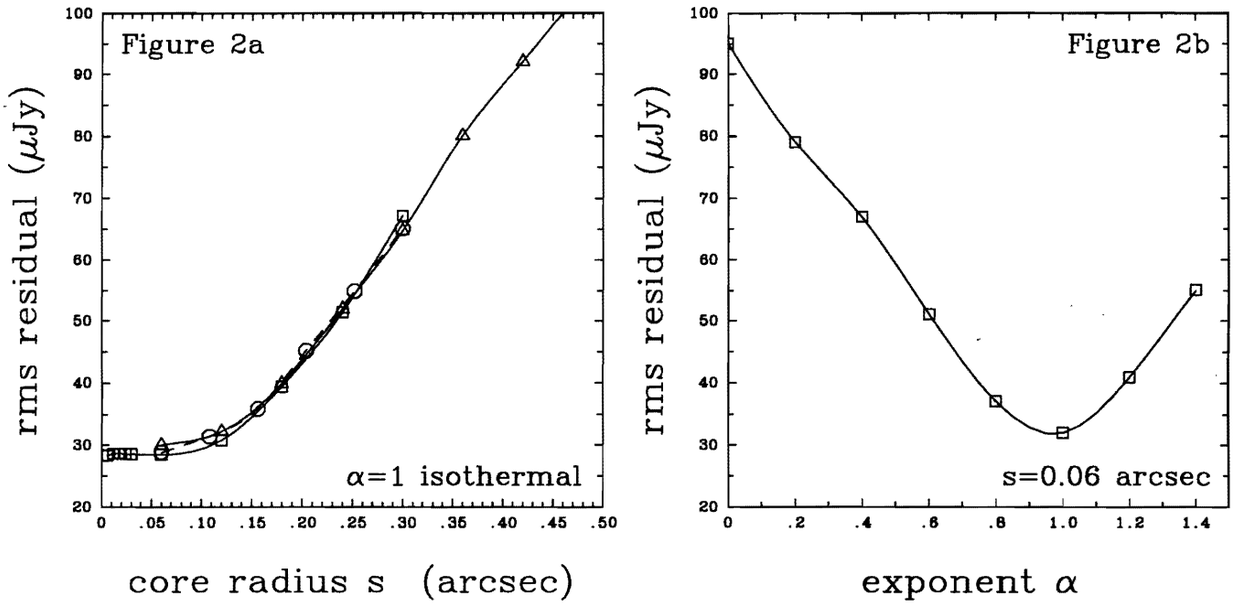

Figure 2: The dependence of the residuals on the core radius s and shape exponent α for the potential $\phi = (b/\alpha)(r^2 + s^2)^{\alpha/2}$ in an external shear field. Figure 2a shows the increase in the residuals as a function of the core radius for several fixed lens positions near the optimal singular isothermal ($\alpha = 1$) model. Figure 2b shows the changes in the residuals as the exponent α is varied for a fixed core radius $s = 0\farcs06$ and lens position near the optimal singular isothermal model. The best fit Plummer models ($\alpha = 0$) have residuals $\sigma \simeq 45\mu$Jy.

the minimum with a quadratic function of the five parameters, $\chi^2 = \chi_0^2 + p_i C_{ij} p_j$ where χ_0^2 is the value at the minimum, then the inverse of C_{ij} is the covariance matrix

$$C_{ij}^{-1} = 10^{-5} \begin{bmatrix} 8.0 & 140 & 140 & -1.0 & -1.6 \\ 140 & 831 & 454 & -2.9 & -3.3 \\ 140 & 454 & 851 & -4.5 & -6.8 \\ -1.0 & -2.9 & -4.5 & 0.031 & 0.028 \\ -1.6 & -3.3 & -6.8 & 0.028 & 0.047 \end{bmatrix}$$

from which we can estimate the errors. The error bar on one parameter p_i (after varying all other parameters to optimize the model) is $\sigma_{p_i} = (C_{ii}\Delta\chi_1^2)^{1/2}$ where the change in the χ^2 for a 99% confidence interval is $\Delta\chi_1^2 = 15.1$. Thus the estimated 99% confidence intervals on the individual parameters are $\sigma_b = 1.0$ mas, $\sigma_x = 10.6$ mas, $\sigma_y = 10.8$ mas, $\sigma_{\epsilon\cos 2\theta_\epsilon} = 0.0022$ and $\sigma_{\epsilon\sin 2\theta_\epsilon} = 0.0027$. Note the large off-diagonal terms in the covariance matrix coupling the lens position to the other three parameters – at a fixed lens position the errors in the other three parameters are small, and most of the variance comes from changes in the parameters as the lens position shifts.

We are currently examining models with a variable core radius and radial profile in an external shear field

$$\phi = \frac{b}{\alpha}\left(r^2 + s^2\right)^{\alpha/2} + \frac{\gamma}{2} r^2 \cos 2(\theta - \theta_\gamma)$$

to estimate the core radius s and shape exponent α of the lens. The singular isothermal version of this model ($\alpha = 1$, $s = 0$) fits the data as well as the truncated elliptical model discussed

above. If we vary the core radius of the isothermal model, we find that the best fit model has no core radius and that the 99% confidence level upper limit on the core radius of $s \lesssim 0\farcs15$, or $s \lesssim 370h^{-1}$ pc in an Einstein-DeSitter universe (see figure 2a). We are in the process of examining the effects of varying α and the initial results suggest that we can rule out more centrally concentrated density profiles, such as a Plummer model ($\alpha = 0$), with a high degree of confidence. As an example, figure 2b shows the variation of the residuals with α for a fixed core radius and lens position. The position is near the optimal isothermal model so it exaggerates the rise in the residuals as α changes, but even the best fit Plummer models ($\alpha = 0$) have residuals of $\sigma \simeq 45\mu$Jy ($\chi^2/\nu \simeq 2.3$). Lens positions along the "bridge" that appears to cross the center of the ring just above the cross in figure 1 catastrophically fail to fit the ring for all values of the parameters.

4 Future Issues

Using LensClean on a cleaned map with the clean beam leads to two ambiguities in estimating the χ^2. The first difficulty is that the residuals left from the original clean can be reduced if the map is recleaned with the compact, Gaussian clean beam – the termination of the original clean only guaranteed that the residuals have little or no correlation with the original, spread-out, dirty beam. This leads to too great a reduction in the residuals in singly imaged regions of the map. The second difficulty, is that the original clean did not interpolate in the missing visibility data consistent with the fact that the object was lensed. When we LensClean the image, we compare not only the true, measured visibilities but also the visibilities interpolated in by Clean. While it is a real requirement that the measured visibilities must be made consistent with the lens model, there is no such requirement on the interpolated visibilities. This means that using the clean map increases the residuals in the multiply imaged regions. We can see an example of this effect in the residual map for MG1654+134 in figure 1. Clean tends to decompose regions of uniform surface brightness into "stripes" of clean components that are then smoothed by the restoring beam. The residual pattern shows exactly this pattern, probably due to how the "stripes" on one side of the ring are being subtracted from the "stripes" on the other side of the ring.

These two effects make the definition of the normalizing residual σ_0 somewhat ambiguous. We also monitor the peak residuals in the inversion, which are insensitive to the over-cleaning of the noise residuals in the singly imaged region. Models with significantly larger rms residuals always have significantly larger peak residuals so the diluting effect of overcleaning the singly imaged region does not seem to affect the results. A temporary solution to this problem is to use the Clean map without the residuals added into it. This prevents LensClean from over subtracting in the singly imaged region without introducing significant errors in the multiply imaged region if the Clean was sufficiently deep and the residuals are dominated by noise. The true solution is to use the raw visibility data produced by the radio arrays rather than the processed Clean maps, and we are slowly developing this approach.

One unpleasant technical issue is that it is hard to simultaneously invert maps made by different interferometer arrays or at different frequencies. The error is sensitive to changes in the position of the lens at the level of 1% of the critical radius or smaller, which is only 10 mas in many of these sources. Misalignments of two maps of the same source at this level can make it impossible to correctly invert both maps simultaneously. This may mean that a small freedom must be left for LensClean to adjust the registration of maps.

Acknowledgements

This research was supported by an Alfred P. Sloan Foundation Fellowship.

References

Clark, B.G., 1980, *A&A* 89, 377
Högbom, J.A., 1974, *A&A Supl* 15, 417
Kochanek, C.S., Blandford, R.D., Lawrence, C.R., & Narayan, R., 1989 *MNRAS* 238, 43
Kochanek, C.S., & Narayan, R., 1992, *Ap J*, 401, 461
Langston, G.I., Connor, S.R., Lehar, J., Burke, B.F., & Weiller, K.W., 1989, *AJ* 97, 1283